Evaluation of the criticality constant from Pulsed Neutron Source measurements in the Yalina-Booster subcritical assembly

V. Bécares[1], D. Villamarín, M. Fernández-Ordóñez[2], E. M. González-Romero

Nuclear Innovation Unit, CIEMAT, Avenida Complutense, 40 - 28040 Madrid (Spain)

C. Berglöf

Department of Reactor Physics, KTH Royal Institute of Technology, Stockholm (Sweden)

V. Bournos, Y. Fokov, S. Mazanik, I. Serafimovich

Joint Institute for Power and Nuclear Research, National Academy of Sciences, Minsk (Belarus)

Abstract

The prompt decay constant method and the area-ratio (Sjöstrand) method constitute the reference techniques for measuring the reactivity of a subcritical system using Pulsed Neutron Source experiments (PNS). However, different experiments have shown that in many cases it is necessary to apply corrections to the experimental results in order to take into account spectral and spatial effects. In these cases, the approach usually followed is to develop different specific correction procedures for each method. In this work we discuss the validity of prompt decay constant method and the area-ratio method in the Yalina-Booster subcritical assembly and propose a general correction procedure based on Monte Carlo simulations.

Keywords: accelerator driven system (ADS), reactivity monitoring, prompt neutron decay constant method, area-ratio (Sjöstrand) method, MCNPX, Yalina-Booster

1. Introduction

Accelerator Driven Systems (ADS) consist in subcritical reactors driven by an external spallation neutron source coupled to a high intensity accelerator. It is widely recognized (Lensa et al. (2008); OECD-NEA (2002, 2006)) that ADS could play an important role in the reduction of the volume and radiotoxicity of high level nuclear waste and therefore make nuclear energy more sustainable.

The development and validation of reactivity monitoring techniques is a key point in the roadmap to a full scale ADS. Hence, a number of experiments have been carried out over the last years in order to evaluate the different techniques of subcriticality monitoring. They include the MUSE (Soule et al. (2004); Villamarín (2004)), TRADE (Jammes et al. (2006)), RACE (Jammes (2007)), Yalina-Thermal (Persson et al. (2005)) and Yalina-Booster (Talamo et al. (2009); Berglöf et al. (2010); Talamo et al. (2012)) experiments. In this paper we focus on the results of the application of Pulsed Neutron Source (PNS) techniques to experiments carried out at the Yalina-Booster subcritical assembly in the framework of the EUROTRANS (IP-Eurotrans (2005)) project of the 6th European Framework Program.

PNS experiments investigate the evolution of the neutron population in the reactor after the injection of very short neutron pulses (ideally instantaneous injection) from an external source. Although this is not intended to be the normal mode of operation of an industrial ADS, which will rather operate in a continuous or quasi-continuous way, PNS experiments are of twofold interest. First, the response of a linear system to such short neutron pulses provides the Green's function (or impulse response) of the system, from which the response of the system to any neutron pulse with arbitrary time dependence can be derived[3]. Second, PNS techniques have already been extensively validated experimentally and thus constitute a reliable starting point for further analysis of reactor kinetics.

Previous experiments have shown that PNS techniques can provide very precise measurements of magnitudes related to the reactivity of the system, such as the prompt neutron decay constant or the prompt-to-delayed area ratio. They have also shown the dependence on the knowledge of the effective kinetic parameters of the system to extract the reactivity from these measurements. However, in most cases, it is very difficult to determine these kinetic parameters from experiments, specially if the system cannot be made critical, so they are obtained from detailed computer simulations of the system.

Furthermore, those experiments have shown that the devia-

[1]corresponding author. Tel: (+34)913460936; Fax: (+34)913466576; vicente.becares@ciemat.es

[2]present address: Tecnatom S.A., Avenida Montes de Oca, 1 - 28703 San Sebastián de los Reyes (Spain)

[3]Assuming that there are neither thermal feedbacks or other elements in the reactor behavior that could limit the linearity of the transport equation.

tion from point kinetics behavior due to local or spectral effects implies additional corrections to obtain unbiased values of the reactivity of the system. Several approaches have been proposed to deal with these effects, such as considering correction factors (Jammes (2007); Talamo et al. (2009); Berglöf et al. (2010); Talamo et al. (2012)), multi-region kinetic models (Villamarín (2004); Jammes et al. (2006); Berglöf et al. (2010)) or using the neutron intergeneration time distribution (Perdu et al. (2003)). However, these approaches are usually specific for either the prompt decay constant or the prompt-to-delayed area ratio reactivity estimators and cannot take into account experimental uncertainties due to composition, geometry or cross sections.

Hence, in this work it is proposed a complete methodology to determine the criticality constant k_{eff} of the system from PNS experiments that takes into account both the spatial and spectral effects present in actual systems and removes the need to know the effective kinetic parameters of the system. This method assumes that, close to the experimental conditions, there is an univocal functional relationship that relates the reactivity of the system and either the prompt decay constant or the prompt to delayed area ratio. These functional relationships can be obtained from simulation using the Monte Carlo code MCNPX (Pelowitz et al. (2005)) by varying different parameters of the system as density, enrichment, geometry and cross sections. In this paper, the Yalina-Booster experiments are used to validate the methodology proposed and the results are compared with previous methods.

2. PNS techniques

A PNS experiment consists in the injection of neutron pulses in the system, repeated at a given frequency, in such a way that the duration of the pulse is shorter than the neutron generation lifetime and the time elapsed between successive pulses is long enough to let prompt neutrons die away. With these conditions, the neutron population in the system will follow an initial fast rise during the introduction of the pulse, then a fast decay driven by prompt neutrons and finally a much slower decay driven by delayed neutrons and their multiplication, that can be approximated by a constant level during the short time between consecutive pulses. An example is shown in figure 1, which corresponds to an actual PNS experiment performed at Yalina-Booster, where the results after many pulses have been averaged in order to improve statistics. In the figure, we can observe the fast decay and the constant level marked with thick lines. In this way, prompt neutron evolution and delayed neutron evolution can be decoupled.

The main techniques available to determine the reactivity of the system from PNS experiments are based in the study of the shape of the prompt neutron decay and the study of the ratio of the areas below prompt neutrons and delayed neutrons.

In the point kinetic model approximation, prompt neutrons decay exponentially and the system reactivity, ρ, can be expressed as function of the decay constant of their population,

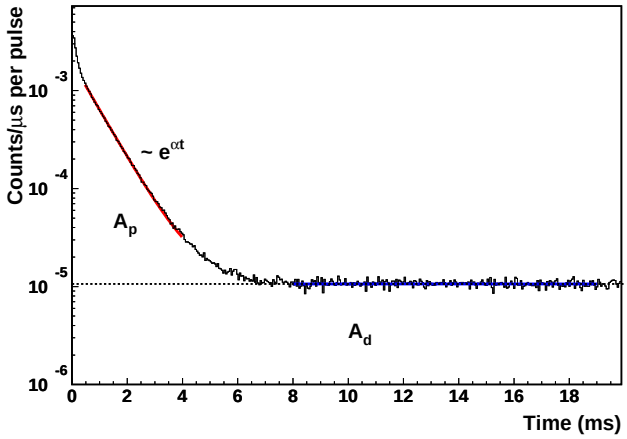

Figure 1: Typical evolution of the counting rate in a detector in the core of Yalina-Booster after a neutron pulse (accumulated for many pulses) with indication of the prompt decay shape and the area ratio methods.

α, as:

$$\frac{\rho}{\beta_{eff}} = \frac{\alpha}{\beta_{eff}/\Lambda_{eff}} + 1 \tag{1}$$

where Λ_{eff} is the effective mean neutron generation time and β_{eff} is the effective delayed neutron fraction. Equation 1 constitutes the basis of the prompt decay constant technique for reactivity determination (Simmonns and King (1958)). Furthermore, the point kinetics model also provides a relationship (Sjöstrand (1956)) between the ratio of the areas under the prompt, A_p, and the delayed, A_d, neutron population evolution curves and the reactivity:

$$\frac{\rho}{\beta_{eff}} = -\frac{A_p}{A_d} \tag{2}$$

In principle, the area ratio technique has the advantage over the prompt decay constant technique that it does not require the knowledge of the kinetic parameter Λ_{eff} to obtain the reactivity in units of dollars. However, it has been shown repeatedly (Soule et al. (2004); Villamarín (2004); Jammes et al. (2006); Jammes (2007); Talamo et al. (2009); Berglöf et al. (2010); Talamo et al. (2012)) that spatial and spectral effects change the the relationship between the measured parameters (α and $\frac{A_p}{A_d}$) and the reactivity of the system. When this occurs, one can expect that non exponential prompt decays are observed or that area ratios differ from one detector position to another. Hence, the estimation of reactivity will be biased and correction methods are needed.

3. The Yalina-Booster subcritical assembly

A schematic view of the Yalina-Booster subcritical assembly (Bournos et al. (2007); Kiyavitskaya et al. (2005)) is presented in figure 2. This assembly consists of a core with two well differentiated regions: a fast spectrum region in the center around

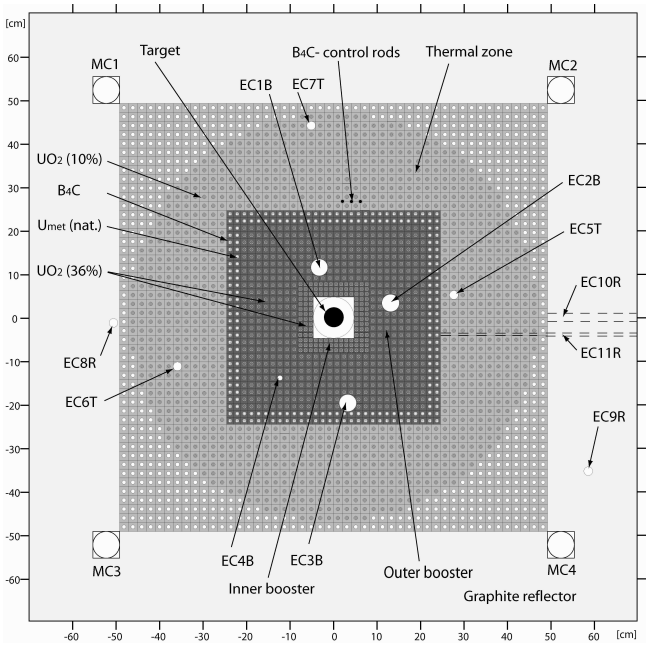

Figure 2: Schematic of the Yalina - Booster subcritical assembly in the SC3a configuration.

the neutron source (known as *booster*) surrounded by a larger thermal spectrum zone, where the essential part of the reactor power is produced. The motivation for this kind of configurations is that the booster can increase the source importance and consequently it could allow reducing the accelerator intensity required for a given power level in the reactor. Such assemblies can be considered as a system of two coupled reactors, being one the booster and the other the thermal zone around it.

During the experiments presented here, the booster was formed by 36% enriched UO_2 fuel rods inserted in lead blocks. The amplification of the neutrons coming from the source is achieved through the fission reactions in the uranium and the (n, xn) reactions in the lead, leading to a fast neutron spectrum. The booster is subdivided in two different regions with different spacing between fuel rods: an inner region with a smaller spacing (inner booster) and an external one with larger spacing (outer booster). The central part contains no fuel and its rear half is empty to hold the neutron source. The zone surrounding the booster is formed by a fuel consisting of mixture of UO_2 (10% enrichment) and Mg in polyethylene blocks which acts as moderator, leading to a thermal neutron spectrum. As stated above, this zone produces most of the power of the reactor. Finally the whole system is radially surrounded by a graphite reflector and axially and radially by a borated polyethylene biological shielding.

A key point in the design of these booster assemblies is the need to prevent, or at least minimize, thermal neutrons from the thermal zone to return back into the booster, partially decoupling the fast and thermal cores. Thus, a so called valve zone formed by thermal neutron absorbers is placed between the booster and the thermal zone. This valve zone consists of an inner layer formed by natural uranium rods and an outer layer formed by B_4C absorbing rods.

Table 1: Core configurations during the experiments: number of fuel pins in each region.

	Inner booster	Outer booster	Thermal zone
SC3a	132	563	1077
SC3b	0	563	1090
SC6	132	563	726

The facility offers great flexibility in core loading patterns, thus allowing different levels of subcriticality by adding or removing fuel rods in the different zones of the assembly. Three experimental configurations, designated SC3a, SC3b and SC6, are considered in this work. SC3a and SC3b were intended to have the same effective multiplication constant of k_{eff}~0.95 but different source multiplications. This is achieved by removing part of the highly enriched uranium of the SC3a inner booster and compensating the decrease of reactivity with more fuel in the periphery. The third configuration (SC6) was intended to have an effective multiplication constant of k_{eff}~0.85, which is a value characteristic of loading or refueling procedures. The composition of the core in each of these configurations is described in table 1. The reactivity can also be slightly changed by using one array of three control rods of B_4C. The values of k_{eff} calculated with MCNPX for these configurations with the control rods inserted and extracted are presented in table 2.

PNS experiments were performed with a (D-T) source, consisting of a tritium target coupled to a 250 keV deuteron accelerator (NG-12-1). The accelerator was operated in pulsed mode at repetition rates of 50 Hz (in the SC3a configuration), 57 Hz (in the SC3b configuration) and 166 Hz (in the SC6 configuration), with pulses of 5 μs of duration and 6 mA of deuteron peak intensity.

Several experimental channels are available at different positions throughout the assembly. The location of these channels is depicted in figure 2. The experimental results presented in this paper were measured with detectors at locations EC1B, EC2B and EC3B in the booster; EC5T and EC6T in the thermal zone and MC2 and MC3 in the reflector. Large (500 mg deposit) U-235 fission chambers (KNT-31) were used in the booster and reflector. In the thermal zone, where the thermal flux was much higher, 1 mg U-235 fission chambers (KNT-5) were used. Peak counting rates during accelerator pulses reached 2×10^6 counts/s in the most sensitive fission chambers. Hence, dead time effects were relevant during the pulse. Dead time is specially relevant to the area-ratio technique, since it requires an accurate determination of A_p. Therefore, experimental counting rates have been corrected to take into account the effect of the dead time.

4. Experimental results

4.1. Prompt decay constant method

Figures 3a, 3b and 3c show the time evolution of the counting rate in a U-235 detector after a D-T pulse in each of the three regions of the assembly: the booster, the thermal zone

and the reflector. The results of the simulations of the counting rates at these positions performed with MCNPX are shown alongside for comparison. In all cases, the constant level due to delayed neutrons has been subtracted. Observing the figures corresponding to the booster and the thermal zone, it can be noticed that after about 1 ms the neutron population decays exponentially. However, in the reflector it takes more time to first rise and then approach an exponential decay.

Equation 1 defines the relationship between the prompt decay constant α and the reactivity ρ in the point kinetics model. Hence, it is possible to perform an exponential fit to the results of each detector in the time region where an exponential decay is observed and use the kinetic parameters β_{eff} and Λ_{eff} to obtain the reactivity. However, as β_{eff} and Λ_{eff} could not be measured experimentally, their values were estimated using the Monte Carlo code MCNPX.

The delayed neutron fraction, β_{eff}, has been computed using the *k-ratio* method (Talamo and Gohar (2010)), also referred as the *prompt method* in Klein Meulekamp and Van der Mark (2006). In this method, β_{eff} is obtained according to equation 3:

$$\beta_{eff} = 1 - \left(\frac{k_p}{k_{eff}}\right)_{MCNPX} \tag{3}$$

where k_p is defined as the effective multiplication factor due to prompt neutrons only, which can be calculated with MCNPX disabling the delayed neutron emission, and k_{eff} is the total effective criticality constant estimation of MCNPX.

On the other hand, the mean neutron generation time, Λ_{eff}, has been calculated using the perturbative methodology proposed in the bibliography (Verboomen et al. (2006)). The results of β_{eff} and Λ_{eff} with different cross sections libraries for the different configurations of Yalina-Booster are listed in table 2.

The prompt decay constants α and the estimated k_{eff} with the ENDF/B-VII.0 nuclear databases are shown in table 3. The results show that the prompt neutron decay constant, and hence the reactivity values, obtained for different detector positions in the fuel region are compatible among each other. Hence, the reactivity estimates are also compatible among themselves. The JEFF-3.1 and JENDL-3.3 databases have also been analyzed and give similar results.

In the reflector region, prompt decay constants show a clear trend to provide lower values than in the fuel region. This indicates that the point kinetics hypothesis is not valid for all detector positions and corrections are required.

It must be also noted that the difference in reactivities due to the control rods insertion, estimated by MCNPX in 305 ± 15 pcm, is clearly noticed and consistent with the calculated values. This shows the high sensitivity of the method and its reliability to estimate reactivity changes of this order of magnitude.

Compared with the simulations, it can be observed that the average experimental k_{eff} are slightly lower (about 300 pcm) than the values calculated with MCNPX (table 2). This is consistent with the larger absolute values of the exponential decay constants in the simulations as noticed in figures 3a and 3b.

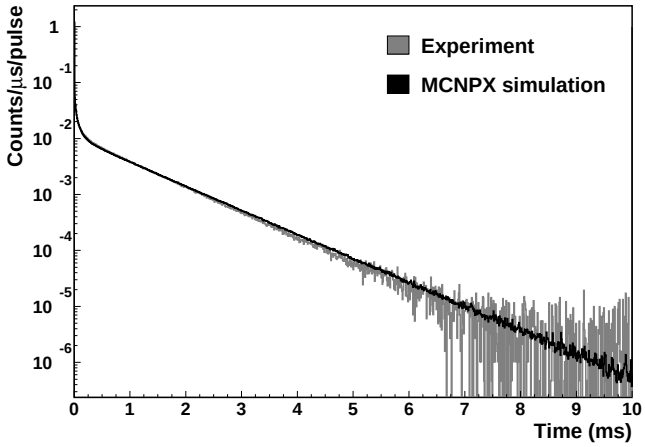

(a) EC1B

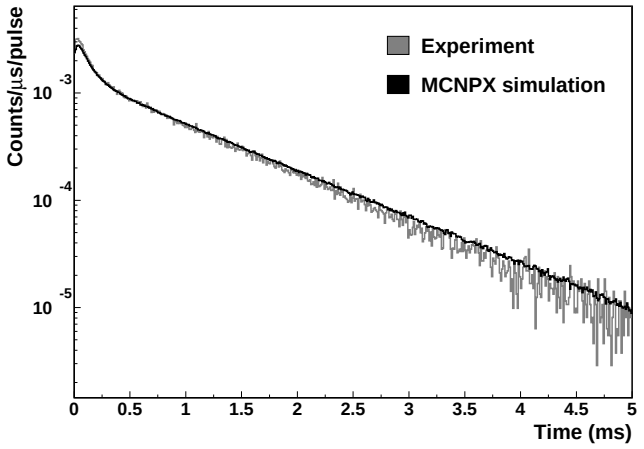

(b) EC5T

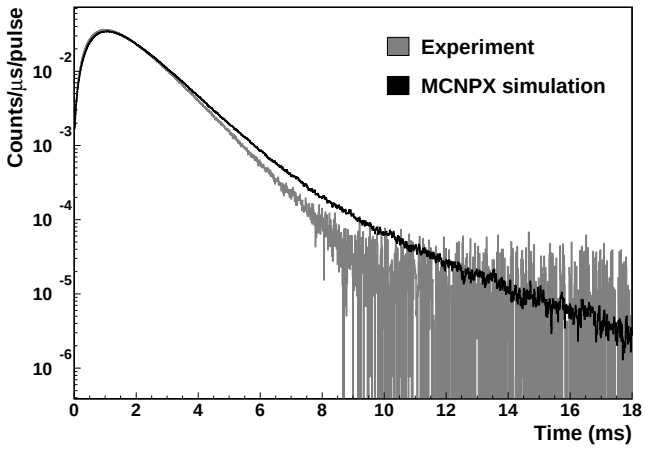

(c) MC2

Figure 3: Evolution of the counting rate after a D-T neutron pulse measured with a U-235 fission chamber in SC3a configuration with the control rods extracted. The result of the MCNPX simulations with the ENDF/B-VII.0 library is included for comparison.

Table 2: Computed k_{eff} and kinetic parameters for the different core configurations of Yalina-Booster.

	Library	k_{eff}, c.r. out	k_{eff}, c.r. in	β_{eff} (10^{-5})	Λ_{eff} (μs)
SC3a	ENDF/B-VII.0	0.94873 ± 0.00011	0.94588 ± 0.00015	729 ± 5	60.8 ± 0.4
	JEFF-3.1	0.94905 ± 0.00004	0.94600 ± 0.00015	747 ± 6	60.8 ± 0.4
	JENDL-3.3	0.94908 ± 0.00011	0.94593 ± 0.00011	734 ± 5	60.9 ± 0.4
SC3b	ENDF/B-VII.0	0.94851 ± 0.00011	0.94544 ± 0.00012	728 ± 6	61.6 ± 0.4
	JEFF-3.1	0.94909 ± 0.00011	0.94584 ± 0.00012	742 ± 6	60.4 ± 0.3
	JENDL-3.3	0.94891 ± 0.00011	0.94601 ± 0.00011	741 ± 6	63.4 ± 0.4
SC6	ENDF/B-VII.0	0.85070 ± 0.00012	—	757 ± 7	67.0 ± 0.5
	JEFF-3.1	0.85133 ± 0.00012	—	772 ± 7	68.1 ± 0.5
	JENDL-3.3	0.85180 ± 0.00010	—	754 ± 7	69.9 ± 0.5

In addition to the direct application of the prompt decay constant method presented in this section, it has been proposed a generalization (Bécares et al. (2010)) of the method that allows the extension of the applicability of the prompt decay constant method beyond the limits of the point kinetics approximation. The extension, that will be denoted as the prompt decay shape method, consists in replacing equation 1 by a general linear relationship between ρ and α:

$$\rho = a\alpha + b \tag{4}$$

where parameters a and b are not necessarily the kinetic parameters Λ_{eff} or β_{eff}. To determine parameters a and b it is necessary the use of simulation codes. In our case, we have used detailed MCNPX simulations where, for simplicity, we have fixed $b = \beta_{\text{eff}}$. In this way, the value of a can be determined from a pair of values (ρ, α) obtained from the simulations. For completeness, we show the results obtained with the prompt decay shape analysis with the ENDF/B-VII.0 database in table 3. Note the similitude of the values of a obtained in this way with the values of Λ_{eff} for all the channels in the core, where the point kinetics is known to be largely valid. The value of a obtained for the reflector is larger, however, and when it is used, the experimental values obtained for k_{eff} with this detector become similar to those obtained with the detectors in the core.

4.2. The area ratio method

The second technique to determine the reactivity from the PNS experiments is the area-ratio technique. As explained in section 2, equation 2 can be used to determine the reactivity of the system from the prompt and delayed counting rate areas. In Yalina-Booster both areas can be easily calculated since the frequency of the neutron pulses is high enough for the delayed neutrons to be considered constant but low enough for the prompt neutrons to decay to negligible values before the following pulse, as shown in figure 1.

The area ratio measured in configurations SC3a, SC3b and SC6 for different detectors is shown in table 4. In this case, the differences in the values among different detectors due to spectral or spatial effects are large (even a factor of two or more) to allow the direct application of the area-ratio method.

A possibility to overcome this problem is the extension of equation 2 using correction factors that relate the prompt to delayed area ratio with the reactivity for every detector position, that is, a relationship of the form:

$$C_{det} = \frac{(A_p/A_d)_{MC}}{|\rho_{MC}|} = \frac{(A_p/A_d)_{MC}}{|\frac{k_{eff,MC}-1}{k_{eff,MC}}|} \tag{5}$$

And the experimental k_{eff} is obtained as:

$$k_{eff,exp} = \frac{1}{1 + \frac{(A_p/A_d)_{exp}}{C_{det}}} \tag{6}$$

A complete discussion of this extension can be found in Berglöf et al. (2010). There, the MCNPX code was used to determine these correction factors for the case of Yalina-Booster. It is worth mentioning that the large spread of k_{eff} estimators was reduced and compatible values were found for all detectors after corrections. We have included the updated results of the application of this technique in table 4 for comparison with the new method we propose in next section.

5. Generalized method

In the previous section, we have shown that in addition to the standard analysis of the experimental results based on the point kinetics approximation, it is possible to extend both the prompt decay constant method and the area ratio method by considering different spatial and spectral effects (equations 4, 5 and 6). These extensions, however, are still based in considering a linear relationship between ρ and the measured quantities, as in the point kinetic model. Furthermore, since a single simulation is used to calculate the parameters in equations 4 and 6, those extensions do not provide a way to estimate the uncertainty or the bias present in the modelization of the experiment.

Hence, we have developed a further generalization of the prompt decay constant and the area ratio methods that takes into account possible inaccuracies in the description of the experiment (geometry, density, composition and cross sections). We propose to relax the conditions given in equations 1 and 2 assuming more general relationships:

$$\rho = \rho_1(\alpha)$$

Table 3: Experimental k_{eff} calculated with the prompt decay constant and the prompt decay shape method in SC3a, SC3b and SC6 configurations with the ENDF/B-VII.0 library. With prompt decay constant method it is meant the direct application of the method, using equation 1 with the experimental values of α and the calculated kinetic parameters (table 2). With prompt decay constant shape it is meant the application using equation 4 with the values of a calculated using MCNPX (also given in the table) and the values of β_{eff} in table 2.

(a) SC3a configuration

Detector position	a (μs)	Control rods out			Control rods in			Δk_{eff}(pcm)	
		α (s^{-1})	k_{eff}, p.d.c	k_{eff}, p.d.s	α (s^{-1})	k_{eff}, p.d.c	k_{eff}, p.d.s	p.d.c	p.d.s
EC1B	61.0 ± 0.2	-1057 ± 3	0.94609 ± 0.00042	0.94595 ± 0.00028	-1128 ± 4	0.94223 ± 0.00045	0.94207 ± 0.00030	387 ± 61	387 ± 41
EC2B	61.0 ± 0.2	—	—	—	-1124 ± 3	0.94249 ± 0.00043	0.94231 ± 0.00027	—	—
EC3B	61.2 ± 0.2	—	—	—	-1097 ± 1	0.94393 ± 0.00040	0.94349 ± 0.00018	—	—
EC5T	61.1 ± 0.2	-1094 ± 8	0.94409 ± 0.00060	0.94381 ± 0.00046	-1134 ± 6	0.94193 ± 0.00051	0.94164 ± 0.00035	216 ± 79	217 ± 58
EC6T	61.2 ± 0.2	—	—	—	-1098 ± 5	0.94385 ± 0.00048	0.94338 ± 0.00031	—	—
MC2	76.2 ± 0.2	-869 ± 4	0.95643 ± 0.00038	0.94437 ± 0.00028	-921 ± 6	0.95354 ± 0.00047	0.94084 ± 0.00042	289 ± 60	353 ± 51

(b) SC3b configuration

Detector position	a (μs)	Control rods out			Control rods in			Δk_{eff}(pcm)	
		α (s^{-1})	k_{eff}, p.d.c	k_{eff}, p.d.s	α (s^{-1})	k_{eff}, p.d.c	k_{eff}, p.d.s	p.d.c	p.d.s
EC1B	61.6 ± 0.3	-1057 ± 7	0.94531 ± 0.00053	0.94530 ± 0.00046	-1143 ± 7	0.94062 ± 0.00057	0.94061 ± 0.00050	469 ± 78	469 ± 68
EC2B	61.7 ± 0.3	-1048 ± 3	0.94581 ± 0.00041	0.94568 ± 0.00032	-1111 ± 3	0.94236 ± 0.00043	0.94222 ± 0.00033	345 ± 59	346 ± 46
EC3B	61.9 ± 0.2	-1043 ± 1	0.94609 ± 0.00039	0.94584 ± 0.00021	-1085 ± 1	0.94377 ± 0.00040	0.94351 ± 0.00021	233 ± 55	234 ± 30
EC5T	61.9 ± 0.2	-1073 ± 6	0.94443 ± 0.00051	0.94414 ± 0.00039	-1125 ± 6	0.94161 ± 0.00054	0.94130 ± 0.00040	282 ± 74	283 ± 56
EC6T	62.0 ± 0.2	-1038 ± 7	0.94639 ± 0.00054	0.94599 ± 0.00043	-1091 ± 7	0.94347 ± 0.00055	0.94304 ± 0.00042	292 ± 77	294 ± 61
MC2	77.2 ± 0.2	-856 ± 4	0.95653 ± 0.00038	0.94445 ± 0.00030	-913 ± 4	0.95334 ± 0.00041	0.94054 ± 0.00033	319 ± 56	390 ± 45

(c) SC6 configuration

Detector position	a (μs)	Control rods out		
		α (s^{-1})	k_{eff}, p.d.c	k_{eff}, p.d.s
EC2B	69.9 ± 2.8	-2624 ± 16	0.85054 ± 0.00124	0.85043 ± 0.00097
EC5T	69.5 ± 3.7	-2659 ± 22	0.84883 ± 0.00143	0.84943 ± 0.00132

Table 4: Experimental values of the prompt to delay area ratio in Yalina-Booster experiments. $k_{eff,direct}$ denotes the values calculated using equation 2 and the ENDF/B-VII.0 values of β_{eff} (table 2). $k_{eff,corr}$ denotes the values calculated using equation 6 and correction factors (C) calculated from simulations using the same library. Different correction factors have been applied for the cases with the control rods inserted and extracted. They are also given in the table.

(a) SC3a configuration

Detector position	Control rods out				Control rods in				Δk_{eff} (pcm)	
	A_p/A_d	C	$k_{eff,direct}$	$k_{eff,corr}$	A_p/A_d	C	$k_{eff,direct}$	$k_{eff,corr}$	direct	corr
EC1B	15.31 ± 0.03	269.58 ± 2.19	0.89960 ± 0.00064	0.94626 ± 0.00045	17.64 ± 0.04	292.83 ± 2.67	0.88606 ± 0.00073	0.94318 ± 0.00053	1354 ± 97	308 ± 70
EC2B	—	244.70 ± 1.83	—	—	15.63 ± 0.03	252.94 ± 2.03	0.89771 ± 0.00065	0.94180 ± 0.00048	—	—
EC3B	—	166.73 ± 1.55	—	—	10.20 ± 0.01	165.11 ± 1.59	0.93079 ± 0.00045	0.94182 ± 0.00056	—	—
EC5T	8.70 ± 0.06	150.26 ± 1.95	0.94036 ± 0.00055	0.94527 ± 0.00080	9.44 ± 0.04	152.91 ± 2.11	0.93561 ± 0.00049	0.94185 ± 0.00084	475 ± 73	342 ± 116
EC6T	—	129.41 ± 1.48	—	—	7.48 ± 0.03	128.86 ± 1.54	0.94829 ± 0.00039	0.94514 ± 0.00069	—	—
MC2	7.23 ± 0.01	125.26 ± 1.39	0.94993 ± 0.00033	0.94543 ± 0.00061	7.85 ± 0.01	129.60 ± 1.55	0.94587 ± 0.00036	0.94289 ± 0.00069	406 ± 49	254 ± 92
MC3	7.24 ± 0.18	126.90 ± 1.41	0.94987 ± 0.00123	0.94578 ± 0.00148	7.88 ± 0.21	125.71 ± 1.57	0.94568 ± 0.00141	0.94102 ± 0.00174	419 ± 187	477 ± 228

(b) SC3b configuration

Detector position	Control rods out				Control rods in				Δk_{eff} (pcm)	
	A_p/A_d	C	$k_{eff,direct}$	$k_{eff,corr}$	A_p/A_d	C	$k_{eff,direct}$	$k_{eff,corr}$	direct	corr
EC1B	15.17 ± 0.03	286.89 ± 3.39	0.90055 ± 0.00076	0.94978 ± 0.00064	17.48 ± 0.09	310.69 ± 4.76	0.88711 ± 0.00097	0.94673 ± 0.00086	1343 ± 123	304 ± 107
EC2B	13.92 ± 0.02	259.96 ± 2.43	0.90799 ± 0.00070	0.94918 ± 0.00048	15.28 ± 0.03	270.41 ± 2.77	0.89990 ± 0.00076	0.94652 ± 0.00056	809 ± 103	266 ± 74
EC3B	9.64 ± 0.01	168.81 ± 1.42	0.93442 ± 0.00051	0.94598 ± 0.00046	10.21 ± 0.01	167.03 ± 1.47	0.93081 ± 0.00053	0.94240 ± 0.00051	361 ± 74	358 ± 69
EC5T	9.26 ± 0.04	151.53 ± 1.85	0.93684 ± 0.00055	0.94241 ± 0.00075	10.07 ± 0.05	153.67 ± 2.00	0.93170 ± 0.00061	0.93850 ± 0.00086	515 ± 82	391 ± 114
EC6T	7.42 ± 0.04	128.17 ± 1.26	0.94875 ± 0.00048	0.94528 ± 0.00061	7.60 ± 0.04	127.74 ± 1.32	0.94757 ± 0.00049	0.94385 ± 0.00065	118 ± 68	143 ± 89
MC2	7.31 ± 0.01	128.38 ± 1.26	0.94947 ± 0.00040	0.94613 ± 0.00053	7.97 ± 0.01	130.52 ± 1.37	0.94516 ± 0.00043	0.94245 ± 0.00061	431 ± 59	368 ± 81

(c) SC6 configuration

Detector position	Control rods out			
	A_p/A_d	C	$k_{eff,exp}$	$k_{eff,corr}$
EC2B	43.63 ± 0.07	268.15 ± 7.74	0.75172 ± 0.00175	0.86006 ± 0.00404
EC5T	23.96 ± 0.85	138.88 ± 6.34	0.84647 ± 0.00476	0.85287 ± 0.00674

and

$$\rho = \rho_2 \left(\frac{A_p}{A_d} \right)$$

The advantage of this methodology is that, even if high spatial modes have a relevant effect in reactor kinetics or there are significant spectral effects on the measurement, such functional relationships may still exist. These relationships can be different for each detector position due to spatial effects, but for being useful for reactivity determination purposes, they must be universal for a certain position. By universal we mean that the same function relates the reactivity ρ and the measurable parameters α or $\frac{A_p}{A_d}$ for any variation of the reactor configuration or of some physical constants. Such a strong hypothesis is not expected to be true for the whole range of configurations and the whole range of reactivities. Nevertheless, we consider that it is reasonable to make a less restrictive hypothesis, and search whether such universal relationship exist for perturbations made around a given configuration with independence of the perturbed parameter.

In the case of Yalina-Booster, the search of this relationship has been performed with a series of simulations of the system using MCNPX. Starting from the most accurate description of configurations, SC3a, SC3b and SC6, we have made small variations of different parameters, namely the polyethylene density, the fuel enrichment and the geometry (height to width ratio). For every variation of these parameters, values of ρ, α and $\frac{A_p}{A_d}$ are calculated. Notice that both α and $\frac{A_p}{A_d}$ are detector dependent. The value of α has been obtained as the decay constant resulting from the fit to an exponential function of the simulated detector counting rate after a neutron pulse for a fixed time interval.

In figure 4, we show the pairs $(\Delta\alpha, \Delta\rho)$ and $\left(\Delta\frac{A_p}{A_d}, \Delta\rho\right)$ obtained in this way for the experimental channels EC1B, EC5T and MC2 for the SC3b configuration. The origin of coordinates corresponds to the non-perturbed configuration using the ENDF/B-VII.0 database. As we can observe, for small variations in the three parameters, there exists a universal relationship between $\Delta\rho$ and either $\Delta\alpha$ or $\Delta\frac{A_p}{A_d}$. Similar results have been obtained for SC3a and SC6.

To remark that the universal relationship between $\Delta\alpha$ and $\Delta\frac{A_p}{A_d}$ with $\Delta\rho$ is only locally true, we have performed large variations of the polythene density. As it can be observed in figure 4, this leads to a multi-valued function for the case of the detectors in the core (EC1B and EC5T), while it remains a well defined linear relationship for the detector in the reflector (MC2). Hence, we have obtained a way to determine the range of validity of the generalized method at different detector positions.

Furthermore, it can be observed in figure 4 that the relationship between $\Delta\rho$ and the measured parameters keeps a good linearity up to about $\Delta\rho = 1000$ pcm. This linearity allows obtaining the reactivity from the experimental measurements with the simple equations:

$$\rho_{exp} = \rho_0 + \Lambda^* \left(\Delta\alpha\right)_{exp} \tag{7}$$

for the case of the generalized version of the prompt decay constant method and

$$\rho_{exp} = \rho_0 + \beta^* \left(\Delta\frac{A_p}{A_d}\right)_{exp} \tag{8}$$

for the case of the generalized version of the prompt to delayed area ratio method. ρ_0 denotes the reactivity of the reference non-perturbed system configuration and the parameters Λ^* and β^* are obtained by the linear fitting of the pairs $(\Delta\alpha, \Delta\rho)$ and $\left(\Delta\frac{A_p}{A_d}, \Delta\rho\right)$, respectively. They have been denoted in this way by analogy with the parameters Λ_{eff} and β_{eff} in equations 1 and 2. The results for Λ^* and β^* obtained with this method are presented in table 5. In principle, the comparison of these parameters with Λ_{eff} and β_{eff} provides a way to estimate the validity of the point kinetics approximation.

In the case of the Λ^* parameter, we observe two different behaviors in Yalina-Booster. First, in the fuel region, where the calculated value of Λ_{eff} is about 15% lower than Λ^* for SC3a and SC3b configurations and 30% in the case of SC6 configuration. This effect is consistent with the fact that point kinetics provides worse results as reactivity lowers. Second, in the reflector region, where the value of Λ^* is very different from Λ_{eff} even for SC3a and SC3b configurations. In this case, the difference is produced by the thermalization in graphite as well as the low absorption cross section.

For its part, the obtained values of β^* vary largely with the detector position. For the case of Yalina-Booster, it is remarkable, however, its nearly positive monotonic tendency from the centermost to the outermost detector position and the tendency to take much lower values than β_{eff} in the booster.

Finally, it is important to remark that the generalized method proposed in this section also provides a way to estimate the systematic uncertainty introduced in the value of k_{eff}. We have adopted the value given by the maximum difference between the mean value of Λ^* and β^* and any of the values of Λ^* and β^* that would be obtained by considering the variation of any of the system parameters (polyethylene density, fuel enrichment, height to width ratio) alone. The uncertainties calculated in this way are presented in table 5. It can be observed that the systematic errors obtained in this way may range from less to 10% to about 50% for the different configurations and detector positions. This variation is to be considered as well to determine the best position for placing a detector for determining the reactivity with the generalized method.

The generalized method provides absolute values for the reactivity, rather than values in units of dollars, without the need of knowing the value of β_{eff}. Therefore, values for k_{eff} can be obtained directly. In table 5 we present the results for k_{eff} obtained with the generalized versions of both the prompt decay constant and the area ratio techniques. It can be observed that the generalized area ratio technique significantly reduces the dispersion of the direct area ratio results. An important remark is that regardless of the k_{eff} absolute values, for a given detector position both methods are capable to clearly noticing the difference in k_{eff} due to the control rods movement. Moreover, when both methods are compared, we also observe that they are compatible.

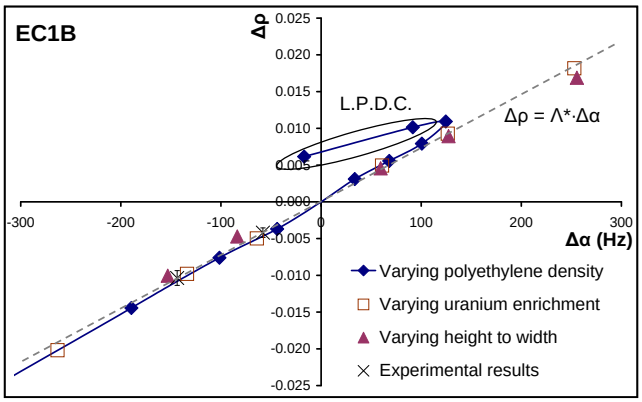

(a) EC1B, prompt decay shape method

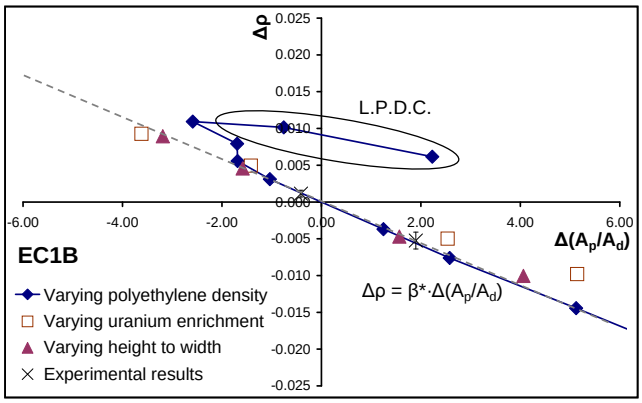

(b) EC1B, area-ratio method

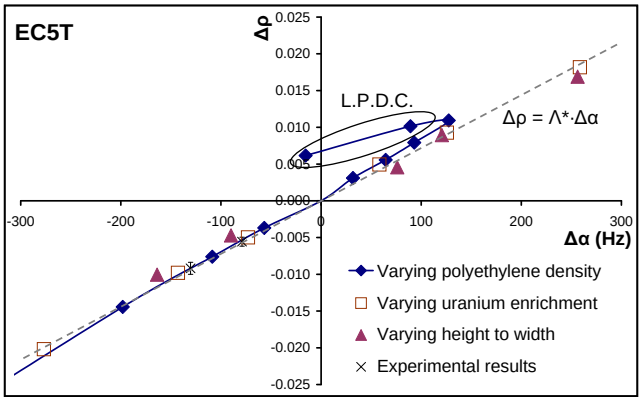

(c) EC5T, prompt decay shape method

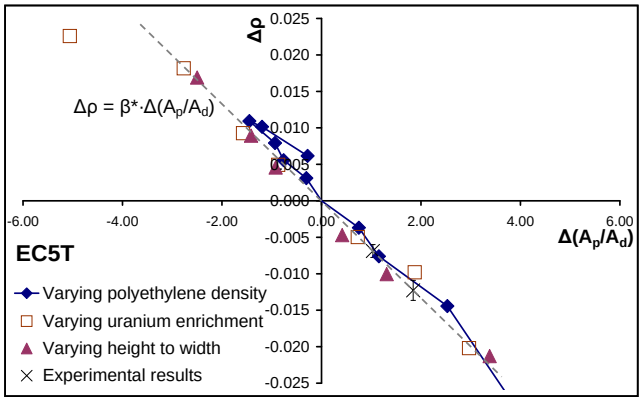

(d) EC5T, area-ratio method

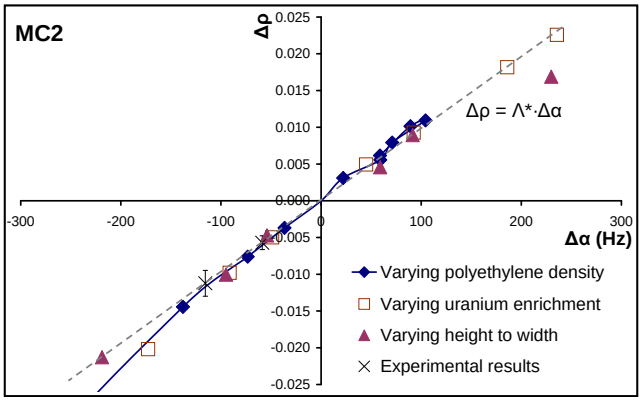

(e) MC2, prompt decay shape method

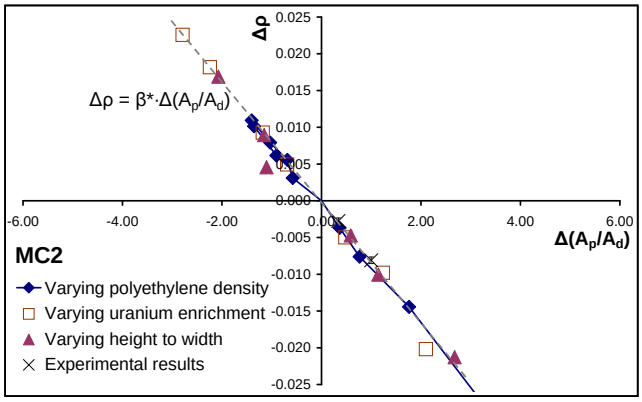

(f) MC2, area-ratio method

Figure 4: $(\Delta\alpha, \Delta\rho)$ and $\left(\Delta(A_p/A_d), \Delta\rho\right)$ values obtained by changing different parameters in the SC3b configuration obtained with the ENDF/B-VII.0 library. The ranges in the variation of the parameters that have been studied are up to ±40% in the polyethylene density, up to ±7.5% in the uranium enrichment and up to ±15% in the height to width ratio. The values corresponding to large polyethylene density changes (L.P.D.C.) are highlighted in the cases where they considerably depart from linearity. The cross sections have also been changed, by considering different nuclear data libraries, but the range of variation is very small in this scale. The dotted lines are the result of fitting these pairs of points to a straight line (in the range where they can be considered to follow a linear relationship). The pairs of points resulting from the application of this generalized method to the experimental values of $(\Delta\alpha, \Delta\rho)$ and $\left(\Delta(A_p/A_d), \Delta\rho\right)$ with the control rods inserted an extracted are also plotted.

Figure 5 shows the results obtained with the generalized method compared with the results of the prompt decay constant and the area ratio techniques (section 4) for the SC3a and SC3b configurations with the control rods inserted and extracted. It is found that the generalized methods, presented in this section, provides very similar k_{eff} results for the prompt decay shape method and the area ratio method using the correction factors presented in section 4. Nevertheless, it can be also observed that the generalized prompt decay shape method tends to slightly shift downwards the results of k_{eff} with respect to the results obtained with the previous version of the prompt decay shape method (equation 4), which may be due to the better account of the spatial and spectral effects that it is in principle allowed with the generalized method.

6. Conclusions

In this work we propose a new methodology to determine the reactivity of a subcritical system. The main hypothesis of this method is that it is always possible to find one or more parameters of the subcritical system, which present a univocal dependence with the reactivity for small variations in the geometry, composition and cross sections. Once such a parameter is found, we can use a simulation code to characterize its dependence with the reactivity.

To check the validity of the new method, we have selected the prompt decay constant and the prompt to delayed area ratio parameters from the point kinetic model. We have then analyzed the experimental results obtained during the Yalina-Booster experiments.

In Yalina-Booster, the presence of an exponential decay mode in the whole fuel zone a few milliseconds after the introduction of an external neutron pulse allows the direct application of the prompt decay constant technique. However, the applicability of this technique in the reflector is limited by the higher order modes that result in a non exponential decay. On the other hand, it has been found that the prompt to delay area ratio is position dependent and the difference in the results can be as large as a factor two.

Hence, it has been possible to demonstrate the capabilities of this new method in an experiment where the point kinetic model parameters (prompt decay constant and prompt to delay area ratio) should have small corrections for the former and strong corrections for the last. In addition to reduce the dispersion in the area ratio estimates of the reactivity, we have shown that it was necessary to shift the estimation of k_{eff} using the prompt decay constant and we have obtained compatible estimation of the reactivity between the two types of observables. The method also provides a way to estimate possible systematic uncertainties. Finally, we have demonstrated that these parameters are sensitive to small variations (control rod insertion) of the reactivity at subcriticality levels expected in ADS.

We consider worth investigating the applicability of this new method in other subcritical experiments with complex kinetic behavior, as it was the case of the MUSE experiment and will be the case of the FREYA experiment of the 7th European Framework Program. If proved valid, they can become useful techniques to determine the reactivity in systems with a strongly space or spectral dependent kinetics.

Acknowledgments

This work was supported by IP-EUROTRANS contract no. FI6W-CT2005-516520; the ENRESA-CIEMAT agreement for the Transmutation Applied to High Level Radioactive Waste; Svensk Kärnbränslehantering AB (SKB, the Swedish Nuclear Fuel and Waste Management Co.) and the Swedish Institute through the Visby program. We also want to thank our colleagues F. Álvarez Velarde and S. Pérez Martín (CIEMAT) for their careful revision of the manuscript.

References

References

Bécares, V., et al., 2010. Correction methods for reactivity monitoring techniques in Pulsed Neutron Source (pns) measurements. In: PHYSOR 2010. Pittsburgh, Pennsylvania, USA, 9–14 May 2010.

Berglöf, C., et al., 2010. Spatial and Source Multiplication Effects on the Area Ratio Reactivity Determination Method in a Strongly Heterogeneous Subcritical System. Nucl. Sci. Eng. 166, 134–144.

Bournos, V., et al., 2007. YALINA-Booster Benchmark Specifications for the IAEA Coordinated Research Projects on Analytical and Experimental Benchmark Analysis on Accelerator Driven Systems, and Low Enriched Uranium Fuel Utilization in Accelerator Driven Sub-Critical Assembly Systems.

IP-Eurotrans, 2005. Annex I - Description of Work. Contract no. FI6W-CT-2004-516520.

Jammes, C., 2007. Analysis of the RACE-LP/IAC experiments. ECATS Deliverable 2.7.

Jammes, C., et al., 2006. Advantages of the area-ratio pulsed neutron source technique for ADS reactivity calibration. Nucl. Instrum. Methods Phys. Res., Sect. A 562, 778–784.

Kiyavitskaya, H., et al., 2005. Experimental investigations at sub-critical facilities of Joint Institute for Power and Nuclear Research - Sosny of the National Academy of Sciences of Belarus. In: Technical Meeting on use of Low Enriched uranium in Accelerator Driven Sub - critical Assemblies. Vienna, Austria, 10–12 Oct 2005.

Klein Meulekamp, R., Van der Mark, S. C., 2006. Calculating the Effective Delayed Neutron Fraction with Monte Carlo. Nucl. Sci. Eng. 152, 142–148.

Lensa, W. v., Nabbi, R., Rossbach, M., 2008. RED-IMPACT - Impact of partitioning, transmutation and waste reduction technologies on the final nuclear waste disposal - Synthesis report. Schriften des Forschungszentrums Jülich - Reihe Energie & Umwelt 15.

OECD-NEA, 2002. Accelerator-Driven Systems (ADS) and fast reactors (FR) in advanced nuclear fuel cycles. A comparative study. Tech. Rep. NEA-3109.

OECD-NEA, 2006. Physics and safety of transmutation systems - A status report. Tech. Rep. NEA-6090.

Pelowitz, D. B., et al., 2005. MCNPX User's Manual. Version 2.5.0. Los Alamos National Laboratory report LA-CP-05-0369.

Perdu, F., et al., 2003. Prompt reactivity determination in a subcritical assembly through the response to a Dirac pulse. Prog. Nucl. Energy 42, 107–120.

Persson, C.-M., et al., 2005. Analysis of reactivity determination methods in the subcritical experiment Yalina. Nucl. Instrum. Methods Phys. Res., Sect. A 554, 374–383.

Simmonns, B. E., King, J. S., 1958. A Pulsed Neutron Technique for Reactivity Determination. Nucl. Sci. Eng. 3, 595–608.

Sjöstrand, N. G., 1956. Measurements on a subcritical reactor using a pulsed neutron source. Ark. Fys. 11, 233–246.

Soule, R., et al., 2004. Neutronic studies in support of accelerator-driven systems: The MUSE experiments in the MASURCA facility. Nucl. Sci. Eng. 148, 124–152.

Table 5: k_{eff} calculated with the generalized method. Upper values have been calculated with the generalized prompt decay shape method and lower values have been calculated with the generalized area-ratio method.

(a) SC3a

Detector position	$\Lambda^*(\mu s)$ / β^* (pcm)	k_{eff}, control rods out	k_{eff}, control rods in	Δk_{eff}(pcm)
EC1B	69.1 ± 9.1	0.94558 ± 0.00051	0.94119 ± 0.00103	438 ± 115
	299 ± 60	0.94674 ± 0.00047	0.94053 ± 0.00165	621 ± 172
EC2B	68.6 ± 9.5	—	0.94151 ± 0.00103	—
	338 ± 77	—	0.94147 ± 0.00166	—
EC3B	69.1 ± 10.3	—	0.94282 ± 0.00089	—
	552 ± 73	—	0.94285 ± 0.00083	—
EC5T	69.2 ± 5.9	0.94316 ± 0.00072	0.94071 ± 0.00077	245 ± 106
	653 ± 68	0.94534 ± 0.00066	0.94104 ± 0.00094	430 ± 114
EC6T	69.8 ± 8.4	—	0.94264 ± 0.00080	—
	787 ± 37	—	0.94529 ± 0.00056	—
MC2	95.5 ± 12.3	0.94326 ± 0.00077	0.93885 ± 0.00135	441 ± 156
	860 ± 5	0.94518 ± 0.00041	0.94044 ± 0.00052	474 ± 66
MC3	*Not enough statistics*			
	839 ± 50	0.94561 ± 0.00142	0.94083 ± 0.00168	478 ± 220

(b) SC3b

Detector position	$\Lambda^*(\mu s)$ / β^* (pcm)	k_{eff}, control rods out	k_{eff}, control rods in	Δk_{eff}(pcm)
EC1B	72.1 ± 5.6	0.94476 ± 0.00059	0.93928 ± 0.00090	548 ± 107
	276 ± 55	0.94954 ± 0.00040	0.94382 ± 0.00102	572 ± 109
EC2B	71.6 ± 5.8	0.94523 ± 0.00043	0.94123 ± 0.00067	401 ± 80
	317 ± 66	0.94908 ± 0.00030	0.94521 ± 0.00074	386 ± 80
EC3B	71.2 ± 5.2	0.94544 ± 0.00030	0.94276 ± 0.00047	268 ± 55
	560 ± 81	0.94611 ± 0.00044	0.94326 ± 0.00080	285 ± 92
EC5T	70.4 ± 5.1	0.94354 ± 0.00055	0.94032 ± 0.00073	322 ± 92
	666 ± 67	0.94236 ± 0.00078	0.93759 ± 0.00120	477 ± 43
EC6T	71.1 ± 7.5	0.94562 ± 0.00057	0.94225 ± 0.00081	337 ± 99
	854 ± 32	0.94497 ± 0.00049	0.94360 ± 0.00050	137 ± 70
MC2	97.1 ± 14.7	0.94340 ± 0.00085	0.93851 ± 0.00155	489 ± 176
	809 ± 19	0.94604 ± 0.00035	0.94129 ± 0.00038	475 ± 52

(c) SC6

Detector position	$\Lambda^*(\mu s)$ / β^* (pcm)	k_{eff}, control rods out
EC2B	112 ± 30	0.85028 ± 0.00156
	360 ± 124	0.85972 ± 0.00404
EC5T	110 ± 29	0.84868 ± 0.00214
	1010 ± 259	0.84876 ± 0.00798

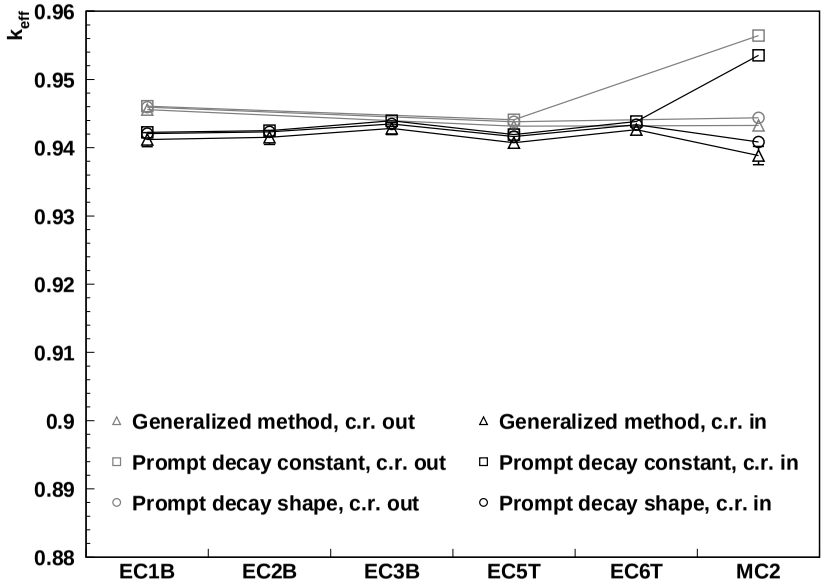

(a) SC3a, prompt decay technique

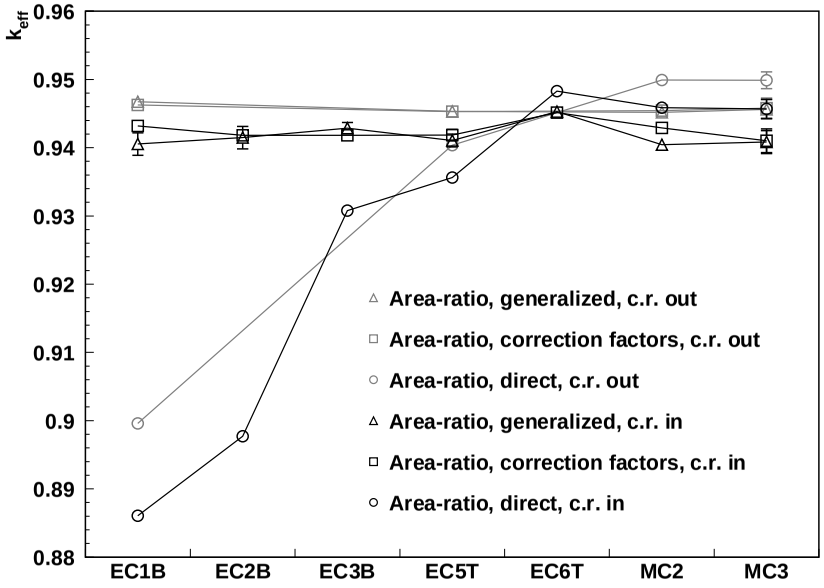

(b) SC3a, area ratio technique

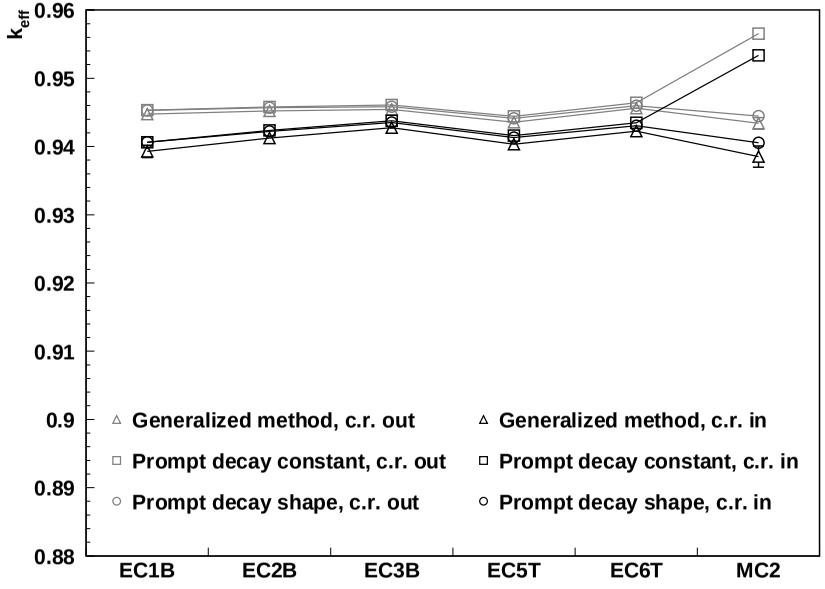

(c) SC3b, prompt decay technique

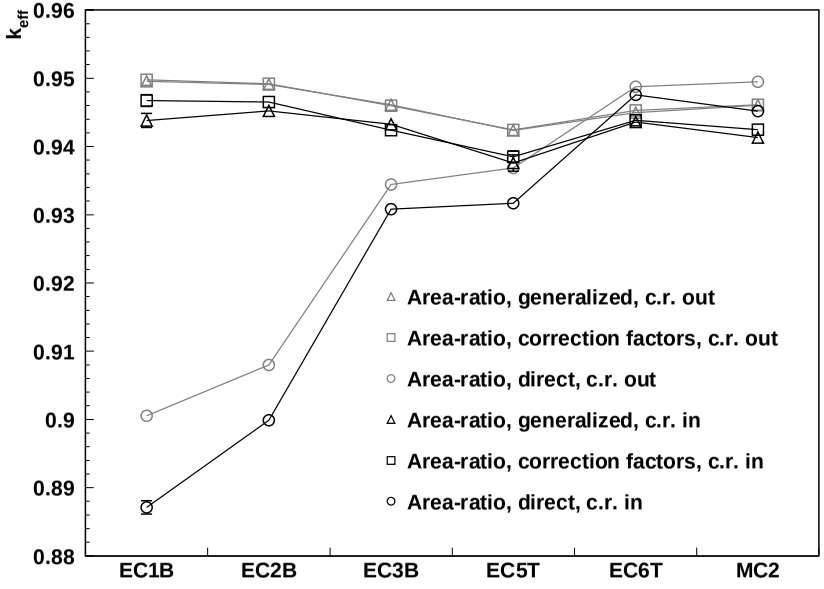

(d) SC3b, area ratio technique

Figure 5: Comparison of the reactivity results obtained with the direct and extended application of both the prompt decay shape and the area ratio techniques for the SC3a and SC3b configurations (all results have been obtained with the ENDF/B-VII.0 library).

Talamo, A., Gohar, Y., 2010. Deterministic and Monte Carlo Modeling and Analyses of Yalina-Thermal Subcritical Assembly. Argonne National Laboratory report ANL-NE-10/17.

Talamo, A., et al., 2009. Pulse superimposition calculational methodology for estimating the subcriticality level of nuclear fuel assemblies. Nucl. Instrum. Methods Phys. Res., Sect. A 606, 661–668.

Talamo, A., et al., 2012. Impact of the neutron detector choice on Bell and Glasstone spatial correction factor for subcriticality measurement. Nucl. Instrum. Methods Phys. Res., Sect. A 668, 71–82.

Verboomen, B., et al., 2006. Monte Carlo calculation of the effective neutron generation time. Ann. Nucl. Energy 33, 911–916.

Villamarín, D., 2004. Análisis dinámico del reactor experimental de fisión nuclear MUSE-4. Ph.D. thesis, Universidad Complutense de Madrid.